



## Abstract

Permafrost distribution modeling in densely populated mountain regions is an important task to support the construction of infrastructure and for the assessment of climate change effects on permafrost and related natural systems. In order to analyze permafrost distribution and evolution on an Alpine-wide scale, one consistent model for the entire domain is needed.

We present a statistical permafrost model for the entire Alps based on rock glacier inventories and rock surface temperatures. Starting from an integrated model framework, two different sub-models were developed, one for debris covered areas (debris model) and one for steep rock faces (rock model). For the debris model a generalized linear mixed-effect model (GLMM) was used to predict the probability of a rock glacier being intact as opposed to relict. The model is based on the explanatory variables mean annual air temperature (MAAT), potential incoming solar radiation (PISR) and the mean annual sum of precipitation (PRECIP), and achieves an excellent discrimination (area under the receiver-operating characteristic, AUROC = 0.91). Surprisingly, the probability of a rock glacier being intact is positively associated with increasing PRECIP for given MAAT and PISR conditions. The rock model was calibrated with mean annual rock surface temperatures (MARST) and is based on MAAT and PISR. The linear regression achieves a root mean square error (RMSE) of 1.6°C. The final model combines the two sub-models and accounts for the different scales used for model calibration. Further steps to transfer this model into a map-based product are outlined.

## 1 Introduction

Today, numerous models exist to estimate the spatial distribution of mountain permafrost in regions of the European Alps (Hoelzle, 1992; Keller, 1992; Imhof, 1996; Gruber and Hoelzle, 2001; Lambiel and Reynard, 2001; Bafu, 2006). These models

TCD

5, 1419–1459, 2011

## Statistical permafrost distribution model

L. Boeckli et al.

Title Page

Abstract

Introduction

Conclusions

References

Tables

Figures

◀

▶

◀

▶

Back

Close

Full Screen / Esc

Printer-friendly Version

Interactive Discussion



follow different empirical or statistical approaches, are calibrated for a certain region and therefore not directly comparable. Further, for large regions in the European Alps the spatial distribution of permafrost is still unknown (e.g., Bavaria, Germany). The objective of the present study is to provide a permafrost distribution model that is designed for a consistent application over the whole European Alps. We decided to use a statistical approach instead of a process-based model because of the limitations of the available calibration and validation data and the complexity of the involved processes. The presented model is based on a Alpine-wide collection of permafrost presence and absence observations (Cremonese et al., 2011). The amount and the spatial distribution of these observations lead to larger ranges in the relevant factors and thus allow new and better analysis than previously possible with regional approaches. Further, our modeling approach distinguishes between two main surface characteristics (cf., Bafu, 2006): debris covered areas (debris model) and steep rock faces (rock model). The calibration data for the two sub-models are rock glacier inventories (debris model) and mean annual rock surface temperature (MARST) measurements (rock model). We offer a framework for the combination of the two sub-models, which use binary (debris model) and continuous (rock model) response variables and are additionally based on different spatial resolutions. The large spatial extent of areas between these to end members of surface domains are treated as a transition zone. This zone could not be directly statistically analyzed for the model because not enough ground truth information was available. It will be addressed using a fusion of the two models. The resulting model predicts a spatially distributed permafrost index based on topo-climatic explanatory variables. Throughout this publication we use an optimistic approach (i.e. having the tendency to over-estimate the amount of permafrost) in line with the aim to provide a model for a warning map informative of possible permafrost. For an unbiased assessment of the total permafrost area, this needs to be re-considered.

The focus of this publication is the analysis of the explanatory variables, the development of the statistical sub-models and their combination. The fitted models are presented in Sect. 5.

**Statistical permafrost  
distribution model**

L. Boeckli et al.

Title Page

Abstract

Introduction

Conclusions

References

Tables

Figures

◀

▶

◀

▶

Back

Close

Full Screen / Esc

Printer-friendly Version

Interactive Discussion



## 2 Background

First attempts to estimate permafrost occurrence in the Alps were based on the so-called “rules of thumb” (Haeberli, 1973), which use basic relations of permafrost occurrence with the topographic attributes altitude, slope angle and slope aspect. These relationships were first implemented within a GIS environment by Keller (1992) and later incorporated in further studies to predict spatial permafrost occurrence (Imhof, 1996; Frauenfelder et al., 1988; Bafu, 2006; Ebohon and Schrott, 2008). Besides topographic variables, climatic information as more direct proxy variables of the surface energy balance (such as MAAT and PISR) is often used in statistical or empirical permafrost models. The basal temperature of snow (BTS), introduced by Haeberli (1975) as an indicator of permafrost occurrence, has been widely used for model assessment (Hoelzle, 1992; Keller et al., 1998; Riedlinger and Kneisel, 2000; Gruber and Hoelzle, 2001; Stocker-Mittaz et al., 2002; Ebohon and Schrott, 2008). Measurements in boreholes and near the ground surface are used for model assessment (Gruber et al., 2004; Heggem et al., 2005; Etzelmüller et al., 2006, 2007; Allen et al., 2009). Other studies use rock glacier inventories to determine the occurrence of permafrost (Janke, 2004), to identify the lower boundary of discontinuous permafrost (Nyenhuis et al., 2005), or for model assessment (Imhof, 1996; Gruber and Hoelzle, 2001).

Existing permafrost distribution models typically do not distinguish between different surface characteristics, even though the thermal coupling and response of ground temperatures to atmospheric conditions and the surface energy balance are significantly influenced by surface cover and timing and thickness of the snow cover. While near-vertical rock faces have a clearly defined interface with the atmosphere where they react directly to changes and heat is predominantly transferred by conduction, ground temperatures in more gentle slopes are connected to atmospheric conditions in a more complex way: thickness and characteristics of the debris cover control the heat transfer in a complex interaction of advection (Delaloye et al., 2003; Juliussen and Humlum, 2008), conduction (Gruber and Hoelzle, 2008) and effects of latent heat. Active layer

### Statistical permafrost distribution model

L. Boeckli et al.

Title Page

Abstract

Introduction

Conclusions

References

Tables

Figures

◀

▶

◀

▶

Back

Close

Full Screen / Esc

Printer-friendly Version

Interactive Discussion





2007, 2008). Consequently, MARST values can indicate permafrost occurrence in the ground. However, MARST values and their extrapolation to subsurface temperatures have to be interpreted with care. Variable thermal conductivity of rock, a thin and discontinuous snow cover and differently fractured surface material can be responsible for a varying thermal offset (Gruber and Haeberli, 2007; Hasler et al., 2011).

### 3 Data

#### 3.1 Response variables

Most of the rock glacier inventories used to set up the debris model were provided by the permafrost observation collection of the project PermaNET (Cremonese et al., 2011). This collection was complemented by inventories from Switzerland published at the Seventh International Conference on Permafrost (“Yellowknife inventories”; ICP Yellowknife, Canada, 23–27 June 1998; Delaloye et al., 1998; Frauenfelder, 1998; Hoelzle, 1998; Imhof, 1998; Phillips, 1998; Reynard and Morand, 1998; Schoeneich et al., 1998) and an inventory from the Upper Engadine Switzerland (Frauenfelder et al., 2001; Frauenfelder, 2005).

For each rock glacier in the PermaNET data set, a polygon defining its boundary and the information concerning its activity is available. The activity information from the different inventories was reclassified into the two classes (1) intact (active, inactive) and (2) relict. The data published in the framework of the 7th ICOP only contains point information from the centroid of the rock glacier. The final data set used as basis for the model development includes 2184 intact and 4193 relict rock glaciers from Austria, France, Italy and Switzerland (Fig. 1).

MARST data were also collected within the Project PermaNET (Cremonese et al., 2011) and include measurements from France, Italy (Pogliotti, 2006; Pogliotti et al., 2008) and Switzerland (PERMOS, 2010; Hasler et al., 2011, Fig. 1). In total, measurements of 57 sensors are used, which are all located in steep rock walls (slope

## Statistical permafrost distribution model

L. Boeckli et al.

Title Page

Abstract

Introduction

Conclusions

References

Tables

Figures

◀

▶

◀

▶

Back

Close

Full Screen / Esc

Printer-friendly Version

Interactive Discussion



inclination  $< 55^\circ$ ) several meters above flat ground to ensure snow-free conditions. The meta-data contains elevation, slope and exposition (measured in the field) as well as the observation period (logger years) taken for the calculation of MARST values. With this information MARST measurements of single years were adjusted to longer term temperature trends according to Allen et al. (2009): longer term mean air temperatures (MAT) from Piz Corvatsch (Upper Engadina, MeteoSchweiz, 2010) for the period 1961–1990 (MAT =  $-6^\circ\text{C}$ ) were compared with mean annual air temperatures (MAAT) of Piz Corvatsch for the period corresponding to the specific logger years. The difference in this two temperatures was used to correct the MARST values. The underlying assumption is that MARST follows MAAT.

### 3.2 Topographic and climatic variables

As potential explanatory variables in our statistical analyses we consider PISR, MAAT, PRECIP, and a seasonal precipitation index (SEASONAL). PISR was derived from the digital elevation model (DEM) ASTER GDEM (Hayakawa et al., 2008) with a grid spacing of 1 arc second (approximately 30 m) using RSAGA (Brenning, 2008) and the algorithm of Wilson and Gallant (2000). PISR was calculated for one year with an hourly temporal resolution and clear sky conditions. The DEM covers the entire Alpine arc and shows an overall accuracy on a global basis of approximately 20 m at 95 % confidence (ASTER, 2009). Alpine-wide MAAT data for the period 1961–1990 (Hiebl et al., 2009) was provided by the Central Institute for Meteorology and Geodynamics (ZAMG, Austria). The MAAT is based on the GTOPO30 elevation model (Center, 1997) with an approximate resolution of 1000 m and shows a monthly standard error of less than  $1^\circ\text{C}$  (Hiebl et al., 2009). A constant lapse rate of  $0.65^\circ\text{C } 100\text{ m}^{-1}$  was used to interpolate the coarse MAAT based on more precise elevation information from the ASTER GDEM. Alpine-wide monthly precipitation data (Efthymiadis et al., 2006) is available for 1800–2003, gridded at 10 min resolution (approximately 15 km, accessible at the ALP-IMP project website: [www.cru.uea.ac.uk/cru/data/alpine/](http://www.cru.uea.ac.uk/cru/data/alpine/)). Based on this data, PRECIP for the period 1961–1990 was calculated. As potential explanatory

## Statistical permafrost distribution model

L. Boeckli et al.

Title Page

Abstract

Introduction

Conclusions

References

Tables

Figures

◀

▶

◀

▶

Back

Close

Full Screen / Esc

Printer-friendly Version

Interactive Discussion



variable for the debris model, PRECIP was centered (cPRECIP) by subtracting its mean value of 1271 mm. Additionally, an index describing the seasonality of precipitation (SEASONAL) was computed by dividing the mean sum of summer precipitation (May–October) by the mean sum of winter precipitation (November–April).

For the locations of the MARST loggers, PISR was calculated based on local terrain measurements (elevation, slope and aspect) according to Corripio (2003), in order to get more precise PISR estimates. Additionally, for the Swiss locations (except the one published by Hasler et al., 2011) local horizons were determined using a camera with fish eye lens (Gruber et al., 2003) and considered in the PISR calculations. Further, the MAAT provided by ZAMG was adjusted for the logger locations using local elevation information measured in the field. The usage of locally measured terrain parameters is necessary for the characterization of MARST, because they strongly depend on high resolution topographic radiation effects such as sun exposure or terrain shading. The resolution of the ASTER GDEM is too coarse for this purpose, but DEMs with very-high resolution and high accuracy, e.g. derived from light detection and ranging (LIDAR) techniques, can be used.

## 4 Statistical methods

### 4.1 Theoretical framework

The theoretical framework is introduced with a general formulation of permafrost distribution models, which allows for a specification in terms of either continuous or binary responses, and a transition between both response types. We then propose a mechanism for integrating the two permafrost models that are based on either rock glacier activity or MARST measurements. We further present an assessment of the possible influence of a change in spatial scale, with particular emphasis on the situation where an empirical model developed using fine-scale in situ measurements (here: MARST and local PISR estimates) is applied at a coarser resolution for regional-scale application.

## Statistical permafrost distribution model

L. Boeckli et al.

Title Page

Abstract

Introduction

Conclusions

References

Tables

Figures

◀

▶

◀

▶

Back

Close

Full Screen / Esc

Printer-friendly Version

Interactive Discussion



## 4.2 Model formulation

Permafrost is defined thermally by the permanent presence of zero or negative ground temperatures ( $^{\circ}\text{C}$ ) over two entire years (van Everdingen, 1998). Because we are interested in depths where the variability of annual ground temperatures can be neglected, we assume maximum ( $\vartheta_{\max}$ ) and mean ( $\vartheta_{\text{mean}}$ ) ground temperatures to be equal. We may therefore express the probability  $p$  of permafrost occurrence at a given location by the probability of mean ground temperature,  $\vartheta_{\text{mean}} = \vartheta$ , being  $\leq 0^{\circ}\text{C}$ :

$$p = P(\vartheta \leq 0) \quad (1)$$

Under the assumption of the ground temperature  $\vartheta$  being normally distributed with a mean value equal to the measurement (or model prediction)  $\bar{\vartheta}$  and a measurement (or prediction) variance  $\sigma_{\vartheta}^2$ , the probability  $p$  can be written as

$$p = \Phi_{\bar{\vartheta}, \sigma_{\vartheta}^2}(-\vartheta), \quad (2)$$

where  $\Phi_{\bar{\vartheta}, \sigma_{\vartheta}^2}$  is the cumulative normal distribution function with mean  $\bar{\vartheta}$  and variance  $\sigma_{\vartheta}^2$ .

If the ground temperature  $\vartheta$  is modeled linearly (as we will later do in the rock model),

$$\vartheta = \tilde{\alpha} + \tilde{\Delta} + \sum_{i=1}^k \tilde{\beta}_i x_i + \tilde{\varepsilon} = \tilde{\vartheta} + \tilde{\varepsilon}, \quad (3)$$

where  $\tilde{\varepsilon}$  is a normally distributed residual error term with mean 0 and variance  $\tilde{\sigma}^2$ , the  $x_i$  and  $\tilde{\beta}_i$  are the model's explanatory variables and their coefficients, and  $\tilde{\alpha} + \tilde{\Delta}$  represents an intercept term that is explained later in detail. In a predictive situation, this model will allow us to predict  $\tilde{\vartheta}$  with a variance  $\tilde{\sigma}_{\text{pred}}^2 \geq \tilde{\sigma}^2$ , which can be estimated from the model. In a predictive situation, the permafrost probability  $p$  is therefore predicted to be

$$p = \Phi(-\tilde{\vartheta} / \tilde{\sigma}_{\text{pred}} > 0). \quad (4)$$

### Statistical permafrost distribution model

L. Boeckli et al.

Title Page

Abstract

Introduction

Conclusions

References

Tables

Figures

◀

▶

◀

▶

Back

Close

Full Screen / Esc

Printer-friendly Version

Interactive Discussion



On the other hand, direct evidence of permafrost presence or absence (debris model) allows us to model the permafrost probability  $p$  directly using generalized linear models with a logistic (e.g., Lewkowicz and Ednie, 2004) or probit link function. Although the logistic link function is more widely used, the probit link function, which is numerically nearly equivalent (Aldrich and Nelson, 1984), is used in this study, because of its relation to the cumulative normal distribution function.

In probit regression (Aldrich and Nelson, 1984), the probability of permafrost presence is modeled linearly not at the probability scale but at the transformed probit scale, which is obtained from an inverse cumulative distribution function of the standard normal distribution:

$$\text{probit}(p) = \Phi^{-1}(p) \quad (5)$$

Thus, and if we introduce an additional (thermal) offset term  $\Delta$  (Sect. 4.3) into the traditional probit model, we write

$$\text{probit}(p) = \alpha + \Delta + \sum_{i=1}^k \beta_i x_i, \quad (6)$$

where the  $x_i$  and  $\beta_i$  are the model's explanatory variables and their corresponding coefficients, and  $\alpha$  is the model intercept.

From Eqs. (4), (5) and (6) it becomes evident that a linear regression of  $\vartheta$  is equivalent to a probit regression of  $p$  with scaled coefficients:

$$-\tilde{\vartheta} / \tilde{\sigma}_{\text{pred}} = \alpha + \Delta + \sum_{i=1}^k \beta_i x_i \quad (7)$$

This relationship between temperature and presence/absence models of permafrost distribution allows us to convert the temperature-based model in Eq. (3) into a probit-based probability model (Eq. 6). It will later be shown that in this specific context, this is relatively insensitive to the estimation of the prediction variance, and we will therefore

**Statistical permafrost distribution model**

L. Boeckli et al.

Title Page	
Abstract	Introduction
Conclusions	References
Tables	Figures
◀	▶
◀	▶
Back	Close
Full Screen / Esc	
Printer-friendly Version	
Interactive Discussion	



use a conservative variance estimator  $\hat{\sigma}_{\text{pred}}^2$ , which will later be specified. The above equivalence allows us to integrate continuous- and binary-response permafrost distribution models within the formal framework of a linear model with comparable model coefficients.

### 4.3 Integration of continuous- and binary-response models

In our case of Alpine-wide permafrost distribution modeling, we wish to integrate two models  $M_\tau$  of permafrost distribution that are fitted separately in two different model domains:  $\tau = d$  (debris surfaces),  $\tau = r$  (exposed steep bedrock) according to the main surface types.

The coefficients of model  $M_d$  are estimated from a generalized linear mixed-effects model of rock glacier activity status (intact versus relict) using a probit link function, resulting in direct estimates of the coefficients  $\alpha_d, \beta_{d,1}, \beta_{d,2}$  adopted from Eq. (6).  $\Delta_d$  is introduced into this model as a fixed offset value that can be used for adjusting effects such as rock glacier movement; this value is not estimated from the data but represents an expert-defined adjustment term.

Model  $M_r$ , by contrast, is fitted indirectly via an ordinary linear regression of rock temperature (Eq. 3) and partly uses the same explanatory variables as model  $M_d$ , with the exception of a difference in spatial scale (discussed in Sect. 4.4). It is important to note that in this model formulation, the adjustment offset  $\hat{\Delta}_r$  can be directly interpreted as a thermal offset of the near-surface ground temperature (MARST) minus the temperature at the top of permafrost (TTOP). Given this model's prediction variance  $\hat{\sigma}_{\text{pred},r}^2$ , we estimate the probit-scale coefficients of  $M_r$  from Eq. (7), i.e. by dividing all temperature-scale model coefficients by  $-\hat{\sigma}_{\text{pred},r}$ .

In practice, the spatial distribution of different surface types is usually not well known and may exhibit transitions such as spatially varying debris or snow cover thicknesses. We represent this in a simple way through a (spatially varying) degree of membership in a land cover class,  $m_\tau$ , with values between 0 and 1 that sum up to 1 at each location.

## Statistical permafrost distribution model

L. Boeckli et al.

Title Page

Abstract

Introduction

Conclusions

References

Tables

Figures

◀

▶

◀

▶

Back

Close

Full Screen / Esc

Printer-friendly Version

Interactive Discussion



The integrated model is then defined to be

$$\text{probit}(\rho_d, \rho_r; m_d, m_r) = m_d \text{probit}(\rho_d) + m_r \text{probit}(\rho_r), \quad (8)$$

which has an obvious generalization to more than two land cover classes. Probabilities of permafrost occurrence can be obtained from this integrated probit value by applying the inverse probit transformation, and probit-scale prediction variances are integrated in a similar way as the weighted sum of each model's prediction variances.

#### 4.4 Scaling issues

While the debris model is based on ASTER GDEM (approximately 30 m resolution) the rock model is calibrated using locally measured terrain attributes, which refer to fine-scale topographic information. When combining these two models we have to consider scale effects and in particular the issue of using different resolutions for model prediction than used for model fitting. With scale effects we refer to the fact that model coefficients may change at different scales or levels of aggregation as coarser-scale explanatory variables tend to show a smaller range of values and less scatter. This situation is related to the change of support problem (e.g., Gotway and Young, 2002), but instead of a geostatistical interpolation setting we need a solution that is tailored to the situation of integrating two linear models.

We start by looking at the scaling problem encountered in the situation where the rock model is fitted at a fine scale (parameters with index "F") and applied at a coarser scale (index "C") and consider initially only a linear model with one explanatory variable ( $k = 1$ ) and no offset term  $\tilde{\Delta}_F = 0$ .

Thus, from Eq. (3),

$$\vartheta_F = \tilde{\alpha}_F + \tilde{\beta}_F X_F + \tilde{\varepsilon}_F, \quad (9)$$

where the residual variance is  $\text{var} \tilde{\varepsilon}_F = \tilde{\sigma}_F^2$ .

Title Page

Abstract

Introduction

Conclusions

References

Tables

Figures

◀

▶

◀

▶

Back

Close

Full Screen / Esc

Printer-friendly Version

Interactive Discussion



In a predictive situation, i.e. at locations other than the measurement sites, we have to approximate the fine-scale  $x_F$  with its coarse-scale equivalent  $x_C$ . We therefore predict  $x_F$  using a scaling model,

$$x_F = f(x_C) + \varepsilon_C, \quad (10)$$

5 where the residuals shall be assumed to be independent and identically distributed according to a normal distribution with mean 0 and variance  $\text{var } \varepsilon_C = \sigma_C^2$ . The function  $f$  represents an arbitrary predictive model, possibly a linear regression in  $x_C$ . More generally, we could approximate  $x_F$  using a model built on possibly multiple variables other than  $x_C$ .

10 Thus,

$$\vartheta_F = \tilde{\alpha}_F + \tilde{\beta}_F f(x_C) + \varepsilon', \quad (11)$$

where the residuals are

$$\varepsilon' = \tilde{\varepsilon}_F + \tilde{\beta}_F \varepsilon_C. \quad (12)$$

15 Since the spatial predictions are to be made at the coarse scale, where one grid cell is composed of  $N$  fine-scale grid cells, we have

$$\vartheta_C = \frac{1}{N} \sum_{i=1}^N \vartheta_F \quad (13)$$

$$= \alpha_F + \tilde{\beta}_F f(x_C) + \frac{1}{N} \sum_i \tilde{\varepsilon}_F + \frac{\tilde{\beta}_F}{N} \sum_i \varepsilon_C, \quad (14)$$

20 where we make use of the fact that  $x_C$  does not vary within a coarse-resolution grid cell. We refer to the last two terms, which involve the fine- and coarse-scale residuals, as the residual of  $\vartheta_C$ .

The estimation of the residual variance of  $\vartheta_C$  is not an easy task because the within-cell residuals  $\tilde{\varepsilon}_F$  and  $\varepsilon_C$ , respectively, can certainly not be considered to be independent because of the likely presence of (positive) spatial autocorrelation over these short

## Statistical permafrost distribution model

L. Boeckli et al.

Title Page

Abstract

Introduction

Conclusions

References

Tables

Figures

◀

▶

◀

▶

Back

Close

Full Screen / Esc

Printer-friendly Version

Interactive Discussion



distances. We argue, however, that it is a conservative choice if we assume that these are in fact mutually independent, which means that we assume that averaging over (small) areal units does not reduce the uncertainty  $\varepsilon'$  in the statistical model of ground temperatures at the aggregated scale. In addition, we replace  $\beta_F^2$  with the square of a one-sided (upper) 95-% confidence limit of  $|\beta_F|$ ,  $\beta_{F,cl}^2$ , where the absolute value expresses that we are using the upper limit away from zero. Thus, as a conservative estimator for  $\text{var}\varepsilon'$ , we use

$$\sigma'^2 := \sigma_F^2 + \beta_{F,cl}^2 \sigma_C^2. \quad (15)$$

Consequently, the residual variance of the scaling model adds to the residual variance of the scaled model, using the regression coefficient for variance weighting, and the equation would be expanded by additional  $\beta_{i,F,cl}^2 \sigma_{i,C}^2$  for each additional explanatory variable to be scaled. Estimates of  $\beta_F$  and  $\sigma_F^2$  can be obtained from the fine-scale rock temperature model, and an estimate of  $\sigma_C$  from the scaling model.

In a predictive situation,  $\sigma_F^2$  can be replaced with the corresponding prediction variance of the rock temperature model, which is generally slightly greater than  $\sigma_F^2$ . The prediction variance varies, however, slightly between samples. In the present study, the prediction variance is inflated only by 6% on average, with a maximum of 11%, and we therefore increase  $\sigma_F^2$  by 6% in general in this study as a first-order approximation.

#### 4.5 Surface types

To distinguish between the two model domains (debris vs. bedrock) one of the following approaches can be applied: (1) an index describing the degree of membership in the exposed bedrock rock surface class, (2) a statistical model of land cover such as a logistic regression or generalized additive model (Hastie and Tibshirani, 1990) or (3) remotely-sensed or map-based land cover products.

## Statistical permafrost distribution model

L. Boeckli et al.

Title Page

Abstract

Introduction

Conclusions

References

Tables

Figures

◀

▶

◀

▶

Back

Close

Full Screen / Esc

Printer-friendly Version

Interactive Discussion



## 4.6 Model fitting and assessment

The debris model is based on a generalized linear mixed-effects model (GLMM) which uses a probit link function to predict the probability of a rock glacier as being intact as opposed to relict (Eq. 6). The GLMM takes into account random inventory effects because the rock glacier inventories are based on different observations techniques and thus lead to heterogeneity in the data. The model is implemented as “glmmPQL” in the R package “MASS” and uses penalized quasi-likelihood for model fitting (Venables and Ripley, 2002). The rock model is based on a linear regression to predict MARST for steep bedrock (Eq. 3).

To assess the accuracy of the probit model (debris model), the area under the receiver-operating characteristics (ROC) curve, which is known as AUROC, was measured. This value ranges between 0.5 (random model behavior) and 1.0 (perfect model). AUROC values reported in this study are based on model predictions that include the inventory random effect. Further, a 10-fold cross-validation (cv) was performed to assess how the model generalizes to independent test data sets. The original data set was randomly partitioned into 10 sub-samples. Of the 10 sub-samples, a single sub-sample was retained for testing the model, and the remaining 9 sub-samples were used as training data. This process was repeated 10 times using each of the 10 sub-samples exactly once as the validation data. The 10 results from the folds were combined to produce a single estimation which then was used to measure the AUROC. The goodness-of-fit for the linear model (rock model) was obtained by measuring the  $R^2$  and the root mean square error (RMSE). Furthermore, the RMSE resulting from a 10-fold cross-validation was calculated.

## 5 Alpine-wide permafrost model

### 5.1 Debris model

The debris model is based on a stratified random sample from the different rock glacier inventories (Sect. 3.1). This results in one spatially random distributed point within the polygon for each rock glacier. For the “Yellowknife inventories”, the centroids of the rock glaciers were used instead, because polygon information was unavailable. Finally, from each of the inventories the same number of intact and relict rock glacier samples was drawn randomly in order to obtain balanced samples. At the end, a total number of 3580 rock glacier points (Table 1) were used. While MAAT and PISR values show a clear relation to the activity of rock glaciers, the correlation with precipitation is less obvious in a univariate analysis (Fig. 2). Nevertheless, cPRECIP was included in the final model based on the high significance of the Wald test (p-value, Table 2). The seasonality of the precipitation (SEASONAL) shows no significant contribution within the debris model (Table 2) and was therefore omitted from the final model.

The chosen GLMM includes MAAT, PISR and cPRECIP as fixed effects and the membership of each point in the different inventories as random effects (Table 2). All explanatory variables show a high significance (p-value). When considering random effects, the debris model achieves an AUROC of 0.91, respective 0.91 for the 10-fold cross-validation, which both are “outstanding” discriminations according to Hosmer and Lemeshow (2000).

The coefficients of the final model indicate: a difference in cPRECIP of 400 mm is empirical identical with a change of 0.52 on the probit scale. A difference in MAAT of 1 °C is equivalent to a probit-change of 0.91. Thus, a change in cPRECIP of 400 mm is identical to a difference in MAAT of 0.57 °C and leads to a dislocation of the limit between intact and relict rock glaciers of 88 m (assuming a constant lapse rate of 0.65 °C 100 m<sup>-1</sup>). An increase of 240 W m<sup>-2</sup> (approximate difference in PISR of a south vs. north exposed slope with an angle of 30°) is associated with a decrease of 1.78 on

TCD

5, 1419–1459, 2011

## Statistical permafrost distribution model

L. Boeckli et al.

Title Page

Abstract

Introduction

Conclusions

References

Tables

Figures

◀

▶

◀

▶

Back

Close

Full Screen / Esc

Printer-friendly Version

Interactive Discussion



the probit scale. This change is equivalent to an increase in MAAT by 1.96 °C or approximately 300 m in elevation.

## 5.2 Rock model

For all 57 locations, MARST are higher than MAAT (Table 3, Fig. 3, left) and the difference between MARST and MAAT increases with higher PISR (Fig. 3, center). PRECIP was not included in the rock model, because the variable shows no high significance and a negative contribution to the Akaike Information Criterion (AIC), which measures model fit while penalizing for model size (Table 4). SEASONAL was omitted from the final model because its range of values on the present training sample was too narrow (from 0.76 to 1.66) to allow for an Alpine-wide application of this empirical relationship (SEASONAL between 0.50 and 2.47).

The coefficients of the chosen model indicate that MARST are generally warmer than the corresponding MAAT. An increase in PISR of 240 W m<sup>-2</sup> is associated with a decrease in MARST of 4.6 °C and is equivalent to a change in MAAT of 4.2 °C. Thus, a change in slope aspect from south to north has a similar influence on MARST as a change in elevation of approximately 650 m.

## 5.3 Scaling model and model combination

A LIDAR DEM covering South Tyrol with a resolution of 2.5 m was used to estimate the prediction variance of the scaling model (data provided by Autonomous Province of Bolzano – South Tyrol, Italy), and the other variance component was estimated from the rock model. PISR derived from the LIDAR DEM refers to local, “real world” estimates and can be compared with PISR values calculated for the rock logger locations.

The following linear regression was fitted to a random sample of 28640 points within South Tyrol above 2000 m and relates finer-scale (2.5-m, LIDAR DEM) PISR to coarse-scale values calculated from a reduced-resolution (30-m, ASTER GDEM) equivalent:

$$\text{PISR}_F = 3.704 + 0.931\text{PISR}_C \quad (16)$$

## Statistical permafrost distribution model

L. Boeckli et al.

Title Page

Abstract

Introduction

Conclusions

References

Tables

Figures

◀

▶

◀

▶

Back

Close

Full Screen / Esc

Printer-friendly Version

Interactive Discussion



The model resulted in an  $R^2 = 0.72$  and a residual standard error of  $46 \text{ W m}^{-2}$ .

For the two other explanatory variables (MAAT and cPRECIP), no scaling correction was necessary because both variables show negligible spatial variation within ASTER GDEM grid cells.

The conservative estimation of  $\sigma'$  (Eq. 15) obtained a value of 1.95 and was used for converting predicted MARST into the corresponding probit-based values (Eq. 7). The individual variance components are displayed in Table (5). The adjustment parameters  $\Delta_r$  (Eq. 3) and the  $\Delta_d$  (Eq. 6) were set to zero which lead to an optimistic estimation of the permafrost occurrence in debris covered areas and a pessimistic one for the rock domain (Sect. 6). Both models (debris and rock model) were then combined using Eq. (8). Probabilities of a rock glacier being intact as opposed to relict, respectively probabilities of  $\text{MARST} \leq 0^\circ\text{C}$  in steep bedrock, were obtained by applying the inverse probit transformation (Fig. 4).

## 6 Discussion

### 6.1 Use and limitations of the model

With the presented approach a consistent permafrost distribution map can be calculated for the entire Alps. The model is based on statistical relations and neglects some of the known physical processes because they could not be resolved in the present data set and models. For example, snow redistribution by avalanche and wind is known to have an impact on mountain permafrost occurrence (Haeberli, 1975; Hoelzle et al., 2001). The explanatory variables MAAT and cPRECIP are derived from existing data sources (Sect. 3.2). PISR estimates are based on a DEM. For an Alpine-wide model application, the ASTER GDEM can be used to calculate PISR values. For regional model application (e.g., South Tyrol, Italy), where more precise DEM data is available, this could be used to derive the PISR values. Functions similar to Eq. (16) are then needed to address the scaling from fine to coarse resolution for the debris model. The prediction is also possible based on two different DEMs: a coarse elevation model

## Statistical permafrost distribution model

L. Boeckli et al.

Title Page

Abstract

Introduction

Conclusions

References

Tables

Figures

◀

▶

◀

▶

Back

Close

Full Screen / Esc

Printer-friendly Version

Interactive Discussion



(e.g., ASTER GDEM) for the debris model representing the mesoscale characteristics of rock glaciers, and a more precise DEM for the rock model because MARST values more strongly depend on accurate PISR estimates. The ASTER GDEM, which is used in this study to calculate PISR and to rescale MAAT for the debris model, shows limitations in the Alps when compared to a more reliable DEM (Frey and Paul, 2011). However, due to the large data sample, these uncertainties are not relevant for Alpine-wide model calibration. Predicting MARST values based on PISR estimates derived from ASTER GDEM is suboptimal, because the ASTER GDEM cannot resolve the small-scale topography well enough.

The statistical relationships are based on indirect permafrost evidence: rock glacier activity as indicator of permafrost existence (intact rock glaciers) or absence (relict rock glaciers) in debris covered areas and negative MARST as a proxy for permafrost occurrence in steep rock walls. To account for the different thermal responses related to surface conditions in these two domains an adjustment offset  $\Delta$  can be applied in our model for each sub-domain model individually (Sect. 4.2). Identifying suitable average adjustment parameters for each domain is challenging because of the large spatial variation of the offsets between different locations (Hoelzle and Gruber, 2008).

The spatial distribution of the rock glaciers used for model calibration (debris model) nearly covers the entire Alps. In contrast, only 57 MARST measurements mostly from the central part of the Alps were available. This inevitably requires a strong generalization of the rock model, especially regarding the precipitation (Sect. 6.2). Further, the temporal extrapolation of MARST values to the period 1961–1990 was addressed by using longterm MAAT measurements. However, the corrected data is sensible to inter-annual variability, because some of the measurement series were only one year long.

The transition zone between debris covered slopes and steep rock walls requires further investigation. Some ground surface temperature (GST) measurements exist in this zone but as mention in Sect. 2 the large inter-annual variability makes this data unsuitable for statistical modeling, which is the reason for not including it in this study.

**Statistical permafrost distribution model**

L. Boeckli et al.

Title Page

Abstract

Introduction

Conclusions

References

Tables

Figures

◀

▶

◀

▶

Back

Close

Full Screen / Esc

Printer-friendly Version

Interactive Discussion



## 6.2 Influence of precipitation

The precipitation variable in the debris model can be seen as a simple proxy for the amount of snow in a regional context or the reduction of short wave insolation by cloud cover. The positive coefficient of the precipitation in the regression model (Sect. 5.1) implies that in areas with higher precipitation, rock glaciers are more likely to be intact, or equivalently, the limit between intact and relict rock glaciers tends to shift towards lower elevations. According to our model, this means that for given MAAT (or elevation in a local context) and PISR conditions, the boundaries of permafrost occurrence in debris-covered and wet areas of the Alps are on average approximately 220 m lower than in relatively dry areas with 1000 mm lower PRECIP. This contrasts with several studies that state that permafrost boundaries are lower in dry or continental areas (e.g., Barsch, 1978; King, 1986), but it is consistent with regional-scale trends in the lower limit of intact rock glacier distribution in the Andes of Central Chile (Brenning, 2005; Azócar and Brenning, 2010). The positive influence of precipitation regarding the intactness of a rock glacier is also shown in Fig. 5, where three different models without precipitation as explanatory variable for drier, normal and relatively wet areas are compared. The three models were calibrated using three sub-samples of the entire data set representing drier, normal and relatively wet inventories. The variable precipitation is not just significant, but also relevant regarding possible model prediction as shown in Fig. 6. The predicted values modeled with cPRECIP as explanatory variable differ with a maximum of 1.5 °C (or approximately 200 m of elevation) from the model prediction without cPRECIP included as explanatory variable.

To further investigate possible relationships between precipitation and the spatial density of rock glaciers, we compared data from two different rock glacier inventories, for which the inventory perimeters were manually digitized (IGUL, Tecino, Switzerland and GEOL, Trentino, Italy); inventory boundaries are currently not available for the other inventories. The results show that rock glacier density in the Alps tends to be higher in areas with less precipitation (Fig. 7). This could explain the widespread notion that also permafrost boundaries occur at lower elevation in dry areas.

### Statistical permafrost distribution model

L. Boeckli et al.

Title Page

Abstract

Introduction

Conclusions

References

Tables

Figures

◀

▶

◀

▶

Back

Close

Full Screen / Esc

Printer-friendly Version

Interactive Discussion



**Statistical permafrost distribution model**

L. Boeckli et al.

[Title Page](#)[Abstract](#)[Introduction](#)[Conclusions](#)[References](#)[Tables](#)[Figures](#)[◀](#)[▶](#)[◀](#)[▶](#)[Back](#)[Close](#)[Full Screen / Esc](#)[Printer-friendly Version](#)[Interactive Discussion](#)

The correlation of MARST and precipitation is weak (Fig. 3, right) and PRECIP shows no significance in the rock model (Table 4). However, the observed significance and magnitude of the influence of SEASONAL suggests that further research on the physical relationship of precipitation seasonality on rock temperatures would be desirable, and that a larger rock temperature data basis would allow us to incorporate an additional relevant predictor variable into the model. According to Gruber et al. (2004) the influence of PISR is larger in dry areas compared to wet areas, especially in south facing rock walls. Seasonal precipitation patterns were not included in the study of Gruber et al.

## 7 Conclusions

The presented empirical approach describes a first Alpine-wide permafrost distribution model. Rock glacier inventories and MARST measurements were used to calibrate the statistical models in two sub-domains (debris cover and exposed bedrock) and both models were combined to predict spatially distributed permafrost probabilities. The model predictions require the availability of (a) PISR estimates, derived from ASTER GDEM or local terrain attributes, (b) MAAT for the period 1961–1990 (Hiebl et al., 2009) and (c) mean annual sum of precipitation for the period 1961–1990 (Efthymiadis et al., 2006).

The debris model uses a generalized linear mixed-effect model with a probit link function to predict the probability of a given rock glacier to be intact as opposed to relict. The influence of precipitation needs further investigations because it conflicts with previous studies. However, this is the first investigation known to the authors, which systematic analyses the spatial rock glacier distribution in relation to precipitation patterns with a large data sample in the Alps (studies exist for the Andes, Brenning, 2005).

The rock model is based on a linear regression and predicts MARST for the period 1961–1990.

Combining two sub-models, which use binary (debris model) and continuous (rock model) response variables and are additionally based on different spatial resolution, needs a land cover map with the surface types: debris and rock cover. The combined model then predicts a uniform permafrost probability. In the debris covered area the model predicts the probability of a rock glacier being intact as opposed to relict. In the rock covered area the model predicts the probability of MARST being  $\leq 0^{\circ}\text{C}$ . For both model domains an offset  $\Delta$ , which may itself be a function of PISR (cf., Hasler et al., 2011), can be introduced in order to account for the different thermal responses related to surface conditions.

The following steps are needed to use the presented approach for Alpine-wide model application and to provide a map-based output product:

- Definition of offset  $\Delta$  for the two different models (rock, debris model).
- Replacement of ASTER GDEM where more precise elevation data is available.
- Providing scaling functions to correct PISR estimates derived from different DEMs.
- Preparation of gridded land cover map with the two classes debris and bedrock slopes.
- Establishment of interpretation guidelines for the map users.

Further we suggest to transform the here presented probabilities to an index, which describes the permafrost occurrence per grid cell discretized in different classes. This index can then be shown in a map, should be consistent for both model domains by using adequate offsets ( $\Delta$ ), and accompanied by interpretation guidelines for local application.

**Statistical permafrost distribution model**

L. Boeckli et al.

[Title Page](#)[Abstract](#)[Introduction](#)[Conclusions](#)[References](#)[Tables](#)[Figures](#)[I◀](#)[▶I](#)[◀](#)[▶](#)[Back](#)[Close](#)[Full Screen / Esc](#)[Printer-friendly Version](#)[Interactive Discussion](#)

*Acknowledgements.* Funding of this study was partly provided by the Alpine Space Program project PermaNET, the Bavarian Environment Agency (Bayerisches Landesamt für Umwelt, LfU), the Swiss Federal Office for the Environment (Bundesamt für Umwelt, BAFU), the Autonomous Province of Bolzano and the Region of Veneto, Geological Survey. Special thanks go to Arthur Lutz and Christian Gschwend for support with data preprocessing. The Swiss Society of Snow, Ice and Permafrost (SEP) as well as The Swiss Geomorphological Society (SGmG) financially supported a research exchange without which this publication would not been possible.

## References

- Aldrich, J. and Nelson, F.: Linear probability, logit, and probit models, Sage Publications, Inc., Beverly Hills, 1984. 1428
- Allen, S., Gruber, S., and Owens, I.: Exploring steep bedrock permafrost and its relationship with recent slope failures in the Southern Alps of New Zealand, *Permafrost Periglac.*, 20, 345–356, doi:10.1002/ppp.658, 2009. 1422, 1425
- ASTER, G.: ASTER Global DEM Validation, Summary Report, Validation Team: METI/ERSDAC, NASA/LPDAAC, USGS/EROS, available at: [http://www.ersdac.or.jp/GDEM/E/image/ASTERGDEM.ValidationSummaryReport\\_Ver1.pdf](http://www.ersdac.or.jp/GDEM/E/image/ASTERGDEM.ValidationSummaryReport_Ver1.pdf), last access: March 2011, 2009. 1425
- Azócar, G. and Brenning, A.: Hydrological and geomorphological significance of rock glaciers in the dry Andes, Chile (27–33° S), *Permafrost Periglac.*, 21, 42–53, doi:10.1002/ppp.669, 2010. 1438
- Bafu: Hinweiskarte der potentiellen Permafrostverbreitung in der Schweiz, Bundesamt für Umwelt (BAFU)/Swiss Federal Office for the Environment, Bern, Switzerland, 2006. 1420, 1421, 1422
- Barsch, D.: Active rock glaciers as indicators for discontinuous alpine permafrost. An example from the Swiss Alps, in: *Proceedings of the 3th International Conference on Permafrost*, Edmonton, Canada, 10–13 July 1978, vol. 1, 349–352, 1978. 1438
- Brenning, A.: Climatic and geomorphological controls of rock glaciers in the Andes of Central Chile: combining statistical modelling and field mapping, Ph.D. thesis, Humboldt-Universität Berlin, Berlin, 2005. 1438, 1439

## Statistical permafrost distribution model

L. Boeckli et al.

Title Page

Abstract

Introduction

Conclusions

References

Tables

Figures

◀

▶

◀

▶

Back

Close

Full Screen / Esc

Printer-friendly Version

Interactive Discussion



**Statistical permafrost distribution model**

L. Boeckli et al.

Title Page

Abstract

Introduction

Conclusions

References

Tables

Figures

◀

▶

◀

▶

Back

Close

Full Screen / Esc

Printer-friendly Version

Interactive Discussion



- Brenning, A.: Statistical geocomputing combining R and SAGA: the example of landslide susceptibility analysis with generalized additive models, *SAGA Seconds Out*, 19, 23–32, 2008. 1425
- Brenning, A., Gruber, S., and Hoelzle, M.: Sampling and statistical analyses of BTS measurements, *Permafrost Periglac.*, 16, 383–393, doi:10.1002/ppp.541, 2005. 1423
- 5 Burn, C. and Smith, C.: Observations of the “thermal offset” in near-surface mean annual ground temperatures at several sites near Mayo, Yukon Territory, Canada, *Arctic*, 41, 99–104, 1988. 1423
- Center, U.: GTOPO30 documentation (README file), Land Processes Distributed Active Archive Center, available at: <http://edcdaac.usgs.gov/GTOPO30/README.asp>, 1997. 1425
- 10 Corripio, J.: Vectorial algebra algorithms for calculating terrain parameters from DEMs and solar radiation modelling in mountainous terrain, *Int. J. Geogr. Inf. Sci.*, 17, 1–23, 2003. 1426
- Cremonese, E., Gruber, S., Phillips, M., Pogliotti, P., Boeckli, L., Noetzi, J., Suter, C., Bodin, X., Crepaz, A., Kellerer-Pirklbauer, A., Lang, K., Letey, S., Mair, V., Morra di Cella, U., Ravanel, L., Scapozza, C., Seppi, R., and Zischg, A.: *Brief Communication: “An inventory of permafrost evidence for the European Alps”*, *The Cryosphere Discuss.*, 5, 1201–1218, doi:10.5194/tcd-5-1201-2011, 2011. 1421, 1424
- 15 Delaloye, R., Reynard, E., and Wenker, L.: Rock glaciers, Entremont, Valais, Switzerland, National Snow and Ice Data Center/World Data Center for Glaciology, Digital Media, Boulder, CO, 1998. 1424
- 20 Delaloye, R., Reynard, E., Lambiel, C., Marescot, L., and Monnet, R.: Thermal anomaly in a cold scree slope (Creux du Van, Switzerland), in: *Proceedings of the 8th International Conference on Permafrost*, Zurich, Switzerland, vol. 1, 175–180, 2003. 1422
- Ebohon, B. and Schrott, L.: Modeling Mountain Permafrost Distribution: a new map of Austria, in: *9th International Conference on Permafrost*, edited by: Kane, D. L. and Hinkel, K. M., Fairbanks, Alaska, Institute of Northern Engineering University of Alaska Fairbanks: Fairbanks, Alaska, 397–402, 2008. 1422
- 25 Efthymiadis, D., Jones, P., Briffa, K., Auer, I., Böhm, R., Schöner, W., Frei, C., and Schmidli, J.: Construction of a 10-min-gridded precipitation data set for the Greater Alpine Region for 1800–2003, *J. Geophys. Res.*, 110, D01105, doi:10.1029/2005JD006120, 2006. 1425, 1439
- 30 Etzelmüller, B., Heggem, E., Sharkhuu, N., Frauenfelder, R., Kääb, A., and Goulden, C.: Mountain permafrost distribution modelling using a multi-criteria approach in the Hövsgöl area, Northern Mongolia, *Permafrost Periglac.*, 17, 91–104, doi:10.1002/ppp.554, 2006. 1422

**Statistical permafrost distribution model**

L. Boeckli et al.

Title Page

Abstract

Introduction

Conclusions

References

Tables

Figures

◀

▶

◀

▶

Back

Close

Full Screen / Esc

Printer-friendly Version

Interactive Discussion



- Etzelmüller, B., Farbroth, H., Gudmundsson, A., Humlum, O., Tveito, O., and Björnsson, H.: The regional distribution of mountain permafrost in Iceland, *Permafrost Periglac.*, 18, 185–199, doi:10.1002/ppp.583, 2007. 1422
- 5 Frauenfelder, R.: Rock glaciers, Fletschhorn Area, Valais, Switzerland, International Permafrost Association, Data and Information Working Group, NSIDC, University of Colorado at Boulder, Boulder, 1998. 1424
- Frauenfelder, R.: Regional-scale modelling of the occurrence and dynamics of rockglaciers and the distribution of paleopermafrost, Ph.D. thesis, Geographisches Institut der Universität Zürich, Zürich, 2005. 1424
- 10 Frauenfelder, R., Allgöwer, B., Haeberli, W., and Hoelzle, M.: Permafrost investigations with GIS – a case study in the Fletschhorn area, Wallis, Swiss Alps, in: Proceedings of the 7th International Conference on Permafrost, Nordicana, Yellowknife, Canada, 23–27 June 1998, 551–556, 1988. 1422
- Frauenfelder, R., Haeberli, W., Hoelzle, M., and Maisch, M.: Using relict rockglaciers in GIS-based modelling to reconstruct Younger Dryas permafrost distribution patterns in the Err-Julier area, Swiss Alps, *Norsk Geogr. Tidsskr.*, 55, 195–202, 2001. 1424
- 15 Frey, H. and Paul, F.: On the suitability of the SRTM DEM and ASTER GDEM for the compilation of topographic parameters in glacier inventories, *Int. J. Appl. Earth Observ. Geoinf.*, submitted, 2011. 1437
- 20 Gotway, C. and Young, L.: Combining incompatible spatial data, *J. Am. Stat. Assoc.*, 97, 632–648, 2002. 1430
- Gruber, S. and Haeberli, W.: Permafrost in steep bedrock slopes and its temperature-related destabilization following climate change, *J. Geophys. Res.*, 112, F02S18, doi:10.1029/2006JF000547, 2007. 1424
- 25 Gruber, S. and Hoelzle, M.: Statistical modelling of mountain permafrost distribution: local calibration and incorporation of remotely sensed data, *Permafrost Periglac.*, 12, 69–77, doi:10.1002/ppp.374, 2001. 1420, 1422
- Gruber, S. and Hoelzle, M.: The cooling effect of coarse blocks revisited: a modeling study of a purely conductive mechanism, in: Proceedings of the 9th International Conference on Permafrost, Fairbanks, Alaska, 30 June–3 July 2008, vol. 1, 557–561, 2008. 1422
- 30 Gruber, S., Peter, M., Hoelzle, M., Woodhatch, I., and Haeberli, W.: Surface temperatures in steep Alpine rock faces – a strategy for regional-scale measurement and modelling, in: Proceedings of the 8th International Conference on Permafrost, Zurich, Switzerland, 21–25

**Statistical permafrost  
distribution model**

L. Boeckli et al.

Title Page

Abstract

Introduction

Conclusions

References

Tables

Figures

◀

▶

◀

▶

Back

Close

Full Screen / Esc

Printer-friendly Version

Interactive Discussion



July 2003, vol. 1, 325–330, 2003. 1423, 1426

Gruber, S., Hoelzle, M., and Haeblerli, W.: Rock-wall temperatures in the Alps: modelling their topographic distribution and regional differences, *Permafrost Periglac.*, 15(3), 299–307, doi:10.1002/ppp.501, 2004. 1422, 1439

5 Haeblerli, W.: Die Basis-Temperatur der winterlichen Schneedecke als möglicher Indikator für die Verbreitung von Permafrost in den Alpen, *Z. Gletscherkunde Glazialgeologie*, IX/1/2, 221–227, 1973. 1422

Haeblerli, W.: Untersuchungen zur Verbreitung von Permafrost zwischen Flüelapass und Piz Grialetsch (Graubünden), *Mitteilungen der Versuchsanstalt für Wasserbau, Hydrologie und Glaziologie der ETH Zürich*, Zurich, Switzerland, 17, 221 pp., 1975. 1422, 1436

10 Harris, S. and Pedersen, D.: Thermal regimes beneath coarse blocky materials, *Permafrost Periglac.*, 9, 107–120, doi:10.1002/(SICI)1099-1530(199804/06)9:2<107::AID-PPP277>3.0.CO;2-G, 1998. 1423

15 Hasler, A., Gruber, S., and Haeblerli, W.: Temperature variability and thermal offset in steep alpine rock and ice faces, *The Cryosphere Discuss.*, 5, 721–753, doi:10.5194/tcd-5-721-2011, 2011. 1423, 1424, 1426, 1440

Hastie, T. and Tibshirani, R.: *Generalized Additive Models*, Chapman & Hall/CRC, London, 1990. 1432

20 Hayakawa, Y., Oguchi, T., and Lin, Z.: Comparison of new and existing global digital elevation models: ASTER G-DEM and SRTM-3, *Geophys. Res. Lett.*, 35, L17404, doi:10.1029/2008GL035036, 2008. 1425

Heggem, E., Juliussen, H., and Etzelmüller, B.: Mountain permafrost in Central-Eastern Norway, *Norsk Geogr. Tidsskr.*, 59, 94–108, doi:10.1080/00291950510038377, 2005. 1422

25 Hiebl, J., Auer, I., Böhm, R., Schöner, W., Maugeri, M., Lentini, G., Spinoni, J., Brunetti, M., Nanni, T., Perčec Tadić, M., Bihari, Z., Dolinar, M., and Müller-Westermeier, G.: A high-resolution 1961–1990 monthly temperature climatology for the greater Alpine region, *Meteorol. Z.*, 18, 507–530, doi:10.1127/0941-2948/2009/0403, 2009. 1425, 1439

Hoelzle, M.: Permafrost occurrence from BTS measurements and climatic parameters in the Eastern Swiss Alps, *Permafrost Periglac.*, 3, 143–147, doi:10.1002/ppp.3430030212, 1992. 1420, 1422

30 Hoelzle, M.: Rock glaciers, Upper Engadin, Switzerland, National Snow and Ice Data Center/World Data Center for Glaciology, Digital Media, Boulder, CO, 1998. 1424

Hoelzle, M. and Gruber, S.: Borehole and ground surface temperatures and their relationship

**Statistical permafrost distribution model**

L. Boeckli et al.

Title Page

Abstract

Introduction

Conclusions

References

Tables

Figures

◀

▶

◀

▶

Back

Close

Full Screen / Esc

Printer-friendly Version

Interactive Discussion



to meteorological conditions in the Swiss Alps, in: Proceedings of the 9th International Conference on Permafrost, Fairbanks, Alaska, 723–728, 2008. 1437

Hoelzle, M., Mittaz, C., Etzelmüller, B., and Haeblerli, W.: Surface energy fluxes and distribution models of permafrost in European mountain areas: an overview of current developments, *Permafrost Periglac.*, 12, 53–68, doi:10.1002/ppp.385, 2001. 1436

Hoelzle, M., Haeblerli, W., and Stocker-Mittaz, C.: Miniature ground temperature data logger measurements 2000–2002 in the Murtèl-Corvatsch area, Eastern Swiss Alps, in: Proceedings of the 8th International Conference on Permafrost, Zurich, Switzerland, 21–25 July 2003, 419–424, 2003. 1423

Hosmer, D. and Lemeshow, S.: *Applied Logistic Regression*, Wiley-Interscience, New York, 2000. 1434

Imhof, M.: Modelling and Verification of the Permafrost Distribution in the Bernese Alps, Switzerland, *Permafrost Periglac.*, 17, 267–280, doi:10.1002/(SICI)1099-1530(199609)7:3<267::AID-PPP221>3.0.CO;2-L, 1996. 1420, 1422, 1423

Imhof, M.: Rock glaciers, Bernese Alps, Western Switzerland, National Snow and Ice Data Center/World Data Center for Glaciology, Digital Media, Boulder, CO, 1998. 1424

Janke, J. R.: The occurrence of alpine permafrost in the Front Range of Colorado, *Geomorphology*, 67, 375–389, doi:10.1016/j.geomorph.2004.11.005, 2004. 1422

Juliussen, H. and Humlum, O.: Thermal regime of openwork block fields on the mountains Elgåhogna and Sølen, Central-Eastern Norway, *Permafrost Periglac.*, 19, 1–18, doi:10.1002/ppp.607, 2008. 1422

Keller, F.: Automated mapping of mountain permafrost using the program PERMAKART within the geographical information system ARC/INFO, *Permafrost Periglac.*, 3, 133–138, doi:10.1002/ppp.3430030210, 1992. 1420, 1422

Keller, F., Frauenfelder, R., Hoelzle, M., Kneisel, C., Lugon, R., Phillips, M., Reynard, E., and Wenker, L.: Permafrost map of Switzerland, in: Proceedings of the 7th International Conference on Permafrost, Nordicana, Yellowknife, Canada, 23–27 June 1998, 557–562, 1998. 1422

King, L.: Zonation and ecology of high mountain permafrost in Scandinavia, *Geograf. Ann. A Phys. Geograph.*, 68, 131–139, 1986. 1438

Lambiel, C. and Reynard, E.: Regional modelling of present, past and future potential distribution of discontinuous permafrost based on a rock glacier inventory in the Bagnes–Heé ré mence area (Western Swiss Alps), *Norsk Geogr. Tidsskr.*, 55, 219–223, 2001. 1420

## Statistical permafrost distribution model

L. Boeckli et al.

Title Page

Abstract

Introduction

Conclusions

References

Tables

Figures

◀

▶

◀

▶

Back

Close

Full Screen / Esc

Printer-friendly Version

Interactive Discussion



Lewkowicz, A. G. and Ednie, M.: Probability mapping of mountain permafrost using the BTS method, Wolf Creek, Yukon Territory, Canada, *Permafrost Periglac.*, 15, 67–80, doi:10.1002/ppp.480, 2004. 1428

MeteoSchweiz: Standardnormwerte 1961–1990: Lufttemperatur 2 m, Schweiz, available at: [http://www.meteoschweiz.admin.ch/web/de/klima/klima\\_schweiz/tabellen.Par.0004.DownloadFile.ext.tmp/temperaturmittel.pdf](http://www.meteoschweiz.admin.ch/web/de/klima/klima_schweiz/tabellen.Par.0004.DownloadFile.ext.tmp/temperaturmittel.pdf), 2010. 1425

Noetzli, J., Gruber, S., Kohl, T., Salzmann, N., and Haeberli, W.: Three-dimensional distribution and evolution of permafrost temperatures in idealized high-mountain topography, *J. Geophys. Res.*, 112, F02S13, doi:10.1029/2006JF000545, 2007. 1423

Noetzli, J., Hilbich, C., Hoelzle, M., Hauck, C., Gruber, S., and Krauer, M.: Comparison of transient 2-D temperature fields with time-lapse electrical resistivity data at the Schilthorn Crest, Switzerland, in: *Proceedings of the 9th International Conference on Permafrost*, Fairbanks, Alaska, 30 June–3 July 2008, 1293–1298, 2008. 1424

Nyenhuis, M., Hoelzle, M., and Dikau, R.: Rock glacier mapping and permafrost distribution modelling in the Turtmantal, Valais, Switzerland, *Z. Geomorphol.*, 49, 275–292, 2005. 1422

Paul, F., Barry, R., Cogley, J., Frey, H., Haeberli, W., Ohmura, A., Ommanney, C., Raup, B., Rivera, A., and Zemp, M.: Recommendations for the compilation of glacier inventory data from digital sources, *Ann. Glaciol.*, 50, 119–126, doi:10.3189/172756410790595778, 2009. 1459

PERMOS: Permafrost in Switzerland 2006/2007 and 2007/2008, edited by: Noetzli, J. and Vonder Muehll, D., *Glaciological Report (Permafrost) No. 8/9 of the Cryospheric Commission of the Swiss Academy of Sciences*, Zurich, Switzerland, 68 pp., 2010. 1423, 1424

Phillips, M.: *Rock Glacier Inventory, Hautes Alpes Calcaires, Switzerland*, National Snow and Ice Data Center/World Data Center for Glaciology, Digital Media, Boulder, CO, 1998. 1424

Pogliotti, P.: *Analisi morfostrutturale e caratterizzazione termica di ammassi rocciosi recentemente deglaciati*, Master's thesis, Earth Science Department, University of Turin, Turin, Italy, 2006. 1424

Pogliotti, P., Cremonese, E., di Cella, U. M., Gruber, S., and Giardino, M.: Thermal diffusivity variability in alpine permafrost rock walls, in: *Proceedings of the 9th International Conference on Permafrost*, Fairbanks, Alaska, 30 June–3 July 2008, vol. 2, 1427–1432, 2008. 1424

Reynard, E. and Morand, S.: *Rock Glacier Inventory, Printse Valley, Valais, Switzerland*, National Snow and Ice Data Center/World Data Center for Glaciology, Digital Media, Boulder, CO, 1998. 1424

Riedlinger, T. and Kneisel, C.: Interaktionen von Permafrost und Ausaperung im Gletschervorfeld des Vadret da Rosatsch, Oberengadin, Schweiz, *Trierer Geograph. Stud.*, 23, 147–164, 2000. 1422

5 Schoeneich, P., Lambiel, C., and Wenker, L.: Rock Glaciers, Prealps, Vaud, Switzerland, National Snow and Ice Data Center/World Data Center for Glaciology, Digital Media, Boulder, CO, 1998. 1424

Stocker-Mittaz, C., Hoelzle, M., and Haeberli, W.: Modelling alpine permafrost distribution based on energy-balance data: a first step, *Permafrost. Periglac.*, 13, 271–282, doi:10.1002/ppp.426, 2002. 1422

10 van Everdingen, R. O.: Multi-Language Glossary of Permafrost and Related Ground-Ice Terms, 25 International Permafrost Association, University of Calgary, Calgary, 1998. 1427

Venables, W. and Ripley, B.: *Modern Applied Statistics with S*, Springer Verlag, New York, 2002. 1433

15 Wilson, J. and Gallant, J.: *Terrain Analysis: Principles and Applications*, John Wiley & Sons, New York, 2000. 1425

---

**Statistical permafrost distribution model**

L. Boeckli et al.

---

Title Page

Abstract

Introduction

Conclusions

References

Tables

Figures

◀

▶

◀

▶

Back

Close

Full Screen / Esc

Printer-friendly Version

Interactive Discussion





## Statistical permafrost distribution model

L. Boeckli et al.

**Table 2.** Model coefficients and standard errors in parentheses of debris models using different sets of explanatory variables, and the corresponding goodness-of-fit statistics. Debris model 2 was chosen as final model.

	Debris model 1	Debris model 2	Debris model 3
Intercept	0.817 (0.192) <sup>***</sup>	0.821 (0.182) <sup>***</sup>	1.366 (0.320) <sup>***</sup>
MAAT	−0.906 (0.046) <sup>***</sup>	−0.882 (0.035) <sup>***</sup>	−0.885 (0.035) <sup>***</sup>
PISR	−0.007 (0.001) <sup>***</sup>	−0.007 (0.001) <sup>***</sup>	−0.007 (0.001) <sup>***</sup>
cPRECIP	0.001 (0.0002) <sup>***</sup>	–	–
SEASONAL	–	–	−0.391 (0.187) <sup>*</sup>
AUROC	0.91	0.90	0.90
AUROC <sub>cv</sub>	0.91	0.91	0.90
Inventory-level standard deviation	0.212	0.413	0.442
Residual standard deviation	1.758	1.377	1.372

Significance of Wald test: \* < 0.05, \*\* < 0.01, \*\*\* < 0.001

[Title Page](#)
[Abstract](#)
[Introduction](#)
[Conclusions](#)
[References](#)
[Tables](#)
[Figures](#)
[I◀](#)
[▶I](#)
[◀](#)
[▶](#)
[Back](#)
[Close](#)
[Full Screen / Esc](#)
[Printer-friendly Version](#)
[Interactive Discussion](#)




## Statistical permafrost distribution model

L. Boeckli et al.

**Table 4.** Model coefficients and standard errors in parentheses of rock models using different sets of explanatory variables, and the corresponding goodness-of-fit statistics. Rock model 2 was chosen as final model.

	Rock model 1	Rock model 2	Rock model 3
Intercept	2.506 (1.006)*	1.677 (0.573)**	2.000 (0.573)***
MAAT	1.055 (0.091)***	1.096 (0.081)***	1.160 (0.083)***
PISR	0.019 (0.002)***	0.019 (0.002)***	0.019 (0.002)***
PRECIP	−0.001 (0.001)	–	–
SEASONAL	–	–	−2.87 (0.943)*
$R^2$	0.82	0.82	0.83
$R^2_{\text{adj}}$	0.81	0.81	0.82
RMSE [°C]	1.56	1.57	1.50
RMSE <sub>cv</sub> [°C]	1.69	1.676	1.65
AIC	222.32	221.39	218.361
Residual standard error [°C]	1.616	1.616	1.561

Significance of Wald test: \* < 0.05, \*\* < 0.01, \*\*\* < 0.001

[Title Page](#)
[Abstract](#)
[Introduction](#)
[Conclusions](#)
[References](#)
[Tables](#)
[Figures](#)
[I◀](#)
[▶I](#)
[◀](#)
[▶](#)
[Back](#)
[Close](#)
[Full Screen / Esc](#)
[Printer-friendly Version](#)
[Interactive Discussion](#)


## Statistical permafrost distribution model

L. Boeckli et al.

Title Page

Abstract

Introduction

Conclusions

References

Tables

Figures

◀

▶

◀

▶

Back

Close

Full Screen / Esc

Printer-friendly Version

Interactive Discussion



**Table 5.** Variance components used for combining the rock and debris models.

	Estimate
$\sigma_F^2 = \text{average}\sigma_{\text{pred}}^2$	2.76
$\beta_{F,cl}$	0.022
$\sigma_C^2$	2108
$\sigma'^2$	3.80

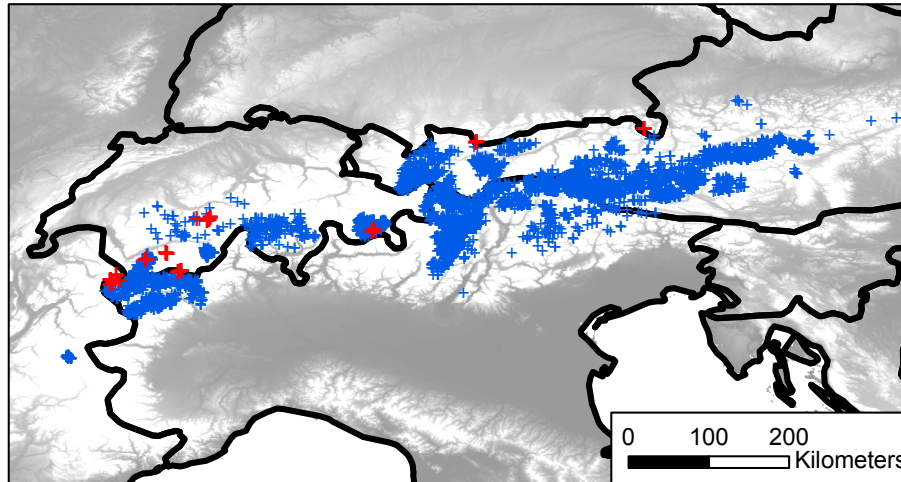


**Fig. 1.** Spatial distribution of intact/relict rock glaciers (blue crosses) and the locations of the rock surface temperature loggers (red crosses).

**Statistical permafrost distribution model**

L. Boeckli et al.

Title Page

Abstract Introduction

Conclusions References

Tables Figures

◀ ▶

◀ ▶

Back Close

Full Screen / Esc

Printer-friendly Version

Interactive Discussion



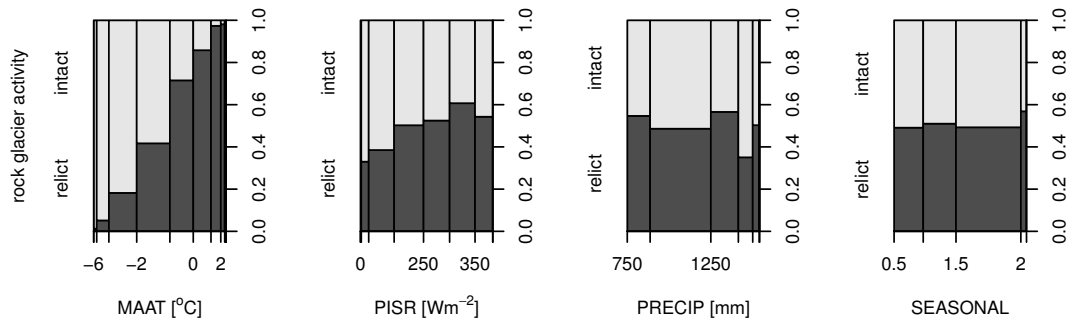


**Fig. 2.** Frequencies of intact as opposed to relict rock glaciers conditional on potential explanatory variables. Bar widths in these spinograms are proportional to the empirical frequency of the given interval of values of explanatory variable. The Figure does not account for random effects.

**Statistical permafrost distribution model**

L. Boeckli et al.

Discussion Paper | Discussion Paper | Discussion Paper | Discussion Paper | Discussion Paper

Title Page

Abstract Introduction

Conclusions References

Tables Figures

◀ ▶

◀ ▶

Back Close

Full Screen / Esc

Printer-friendly Version

Interactive Discussion



**Statistical permafrost  
distribution model**

L. Boeckli et al.

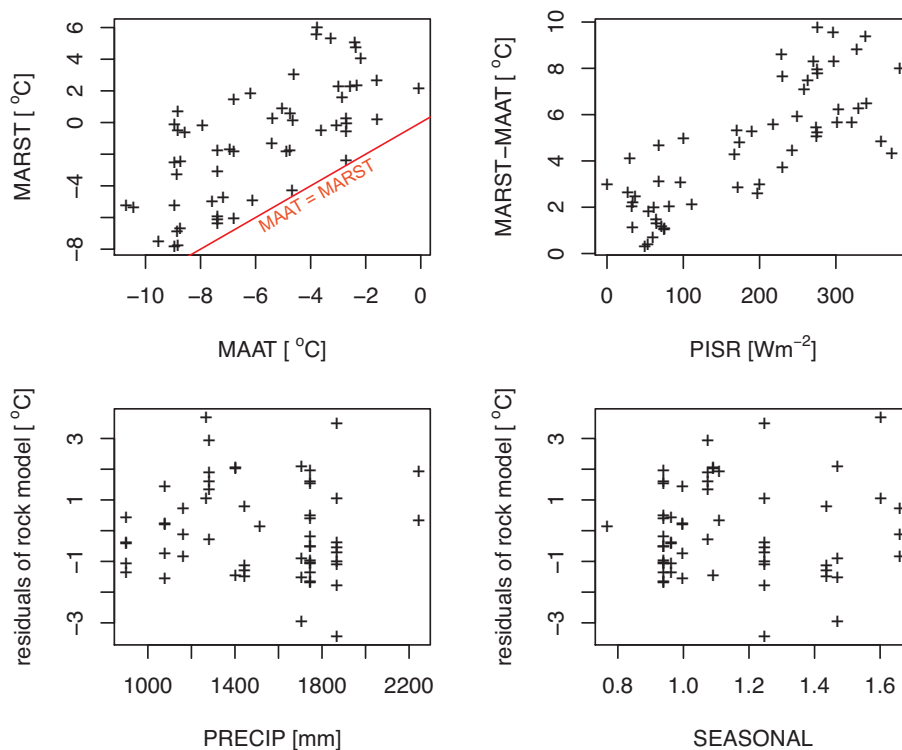


**Fig. 3.** Scatterplots illustrating the relation of MARST to MAAT (top left) and of the difference between MARST and MAAT to PISR (top right) for the 57 MARST loggers. In the lower panels, the model residuals of the rock model are plotted against PRECIP and SEASONAL to visualize possible relations of these two variables.

[Title Page](#)[Abstract](#)[Introduction](#)[Conclusions](#)[References](#)[Tables](#)[Figures](#)[◀](#)[▶](#)[◀](#)[▶](#)[Back](#)[Close](#)[Full Screen / Esc](#)[Printer-friendly Version](#)[Interactive Discussion](#)

**Statistical permafrost  
distribution model**

L. Boeckli et al.

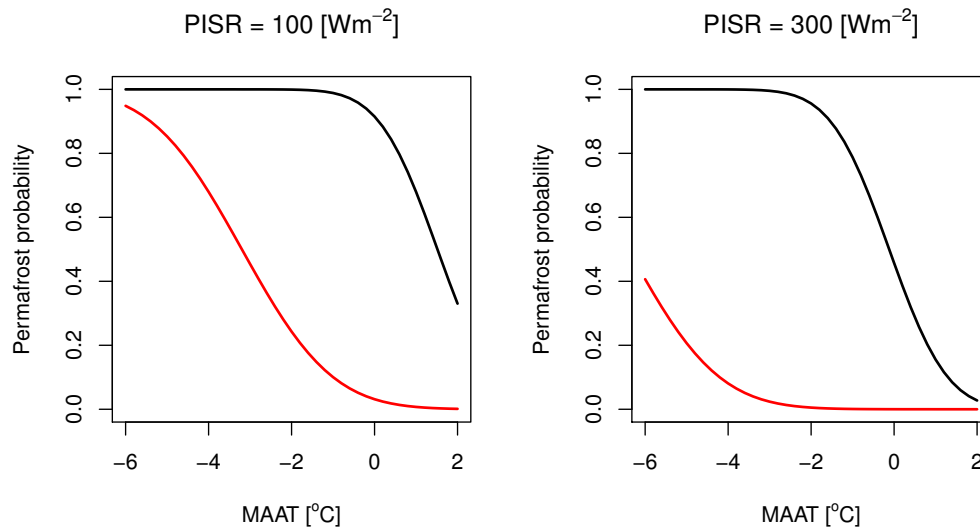


**Fig. 4.** Predicted probabilities of a rock glacier being intact (black) and of  $\text{MARST} \leq 0^\circ\text{C}$  in steep bedrock (red). A precipitation value of 1271 mm ( $\text{cPRECIP} = 0$  mm) was used for both plots.

[Title Page](#)[Abstract](#)[Introduction](#)[Conclusions](#)[References](#)[Tables](#)[Figures](#)[◀](#)[▶](#)[◀](#)[▶](#)[Back](#)[Close](#)[Full Screen / Esc](#)[Printer-friendly Version](#)[Interactive Discussion](#)

Statistical permafrost distribution model

L. Boeckli et al.

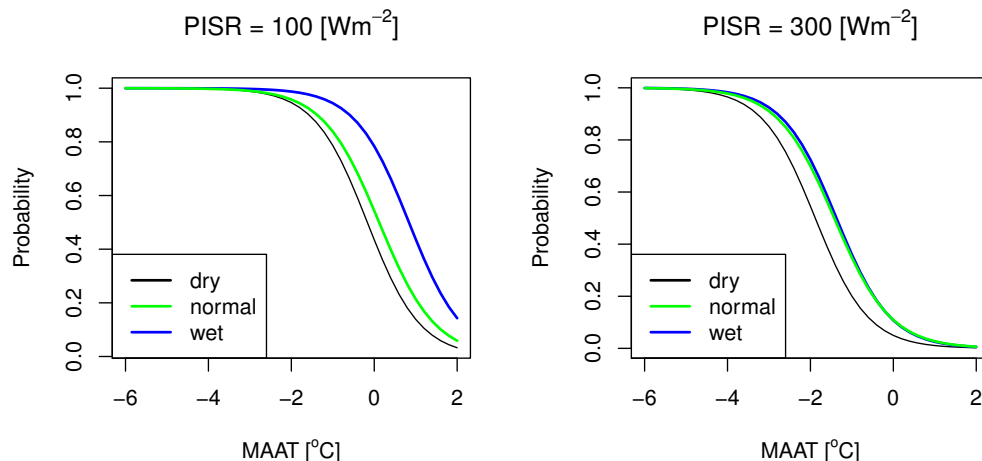


**Fig. 5.** Probabilities of a rock glacier being intact as opposed to relict for drier (mean PRECIP = 1105 mm), normal (mean PRECIP = 1291 mm) and relatively wet (mean PRECIP = 1679 mm) inventories using three different models (dry, mean, wet). The three models do not include cPRECIP as explanatory variable.

Discussion Paper | Discussion Paper | Discussion Paper | Discussion Paper | Discussion Paper

Title Page	
Abstract	Introduction
Conclusions	References
Tables	Figures
◀	▶
◀	▶
Back	Close
Full Screen / Esc	
Printer-friendly Version	
Interactive Discussion	



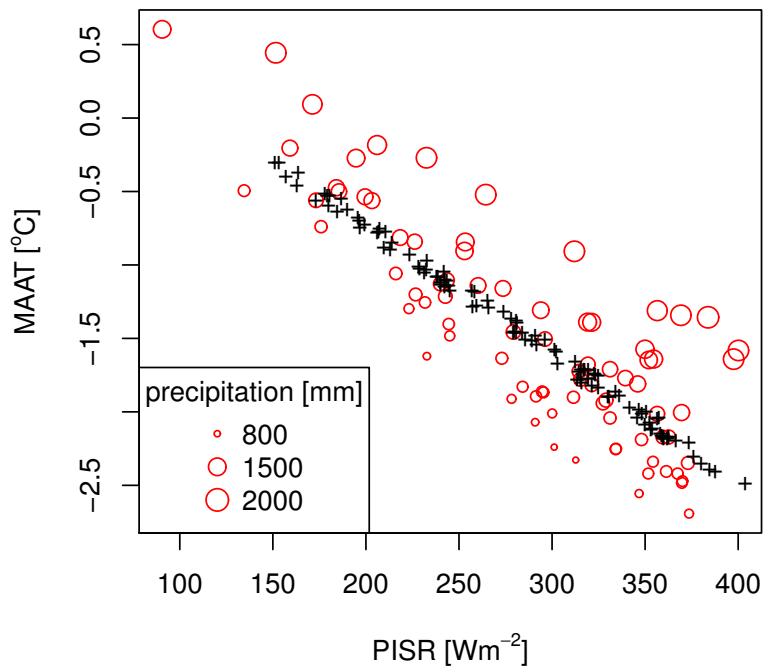


**Fig. 6.** Prediction values for the two first models from Table 2 calculated for a randomly selected probability range of 0.475–0.525 for intact rock glacier occurrence. Black crosses: debris model without cPRECIP as explanatory variable, red bubbles: debris model including cPRECIP as explanatory variable.

**Statistical permafrost distribution model**

L. Boeckli et al.

Title Page	
Abstract	Introduction
Conclusions	References
Tables	Figures
◀	▶
◀	▶
Back	Close
Full Screen / Esc	
Printer-friendly Version	
Interactive Discussion	



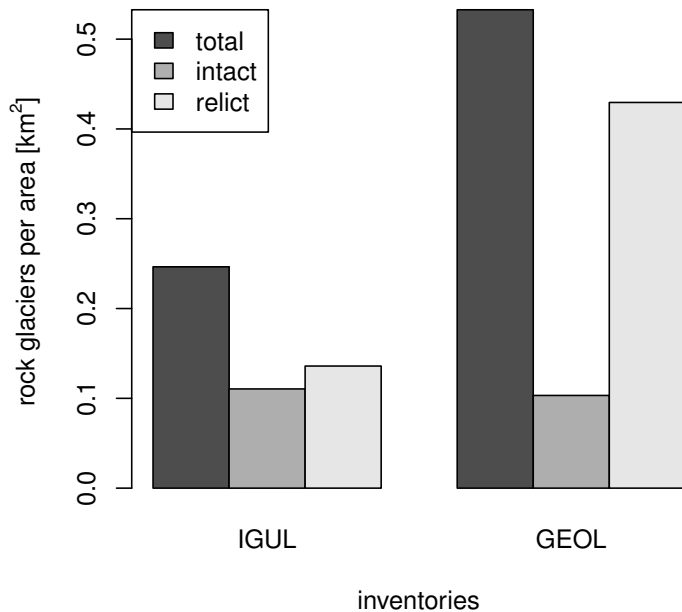


**Fig. 7.** Spatial density of rock glacier occurrence in a wet (IGUL Tecino, Switzerland; mean PRECIP = 1900 mm) and a dry (GEOL, Trentino, Italy; mean PRECIP = 1072 mm) inventory. The relevant area is calculated for areas above 2000 m of elevation excluding glaciated areas (data provided by Paul et al., 2009) and steep slopes (slope < 50°).

**Statistical permafrost distribution model**

L. Boeckli et al.

Title Page

Abstract Introduction

Conclusions References

Tables Figures

◀ ▶

◀ ▶

Back Close

Full Screen / Esc

Printer-friendly Version

Interactive Discussion

